

Exploring the optimal dose of low ionizing radiation to enhance immune function: a rabbit model

Yuhong Zhang¹, Hongyan Ren¹, Yifan Zheng¹,
Qiang Yang¹, Miao Li¹, Hongqian Gu² and
Liguo Hao² 

Abstract

Primary liver cancer is one of the most common malignant tumors in China. Currently, immunotherapy for liver cancer is a research hotspot. Experimental studies and epidemiological investigations have confirmed the antineoplastic activity of low ionizing radiation. The aim of this study was to explore the optimal dose of low ionizing radiation to enhance immune function. Twenty-five New Zealand rabbits were randomly divided into five groups (n = 5 each): experimental group 1 (25 mGy), experimental group 2 (50 mGy), experimental group 3 (75 mGy), experimental group 4 (100 mGy), and the control group (0 mGy). VX-2 tumor tissue was injected into rabbits using a high-frequency B-ultrasound probe (3.5 MHz). Rabbits were irradiated, and on day 4 after irradiation, blood was collected from each rabbit. Blood chemistry, interleukin (IL)-4, interferon (IFN)- γ , immunoglobulin (Ig)G, and IgM levels were assessed. On day 15 after irradiation, macrophage phagocytic function was assessed. The rabbits were sacrificed, and the spleen was removed and weighed to calculate its spleen index. Each parameter was highest in the experimental group 3 (75 mGy). Thus, we suspect the optimal low ionizing radiation dose to improve immune function may be 75 mGy.

¹Medical Imaging Class 17-03, School of Medical Technology, Qiqihar Medical University, Heilongjiang, Qiqihar, China

²Molecular Imaging Laboratory, School of Medical Technology, Qiqihar Medical University, Heilongjiang, Qiqihar, China

Corresponding author:

Liguo Hao, Molecular Imaging Laboratory, School of Medical Technology, Qiqihar Medical University, No. 333 Bu Kui North Street, Jianhua District, Qiqihar, Heilongjiang 161000, China.
Email: haoliguo@qmu.edu.cn



Keywords

Primary liver cancer, rabbit model, low ionizing radiation, immune function, immunoglobulin M, immunoglobulin G

Date received: 9 October 2020; accepted: 14 April 2021

Introduction

Primary liver cancer (hereafter referred to as liver cancer) is the fourth most common malignant tumor in China, with the highest morbidity and mortality rate and a yearly increasing trend, and it poses a great threat to the health of Chinese people.^{1,2} Considering the complexity of tumor biology in liver cancer and the limitations of various treatment methods, multidisciplinary cooperation and the use of multiple treatment methods is required to treat liver cancer. With the rapid development of modern medical cellular immunity and biomolecule technology, biotherapy has become an important method to treat liver cancer. Tumor biotherapy is the application of biological technologies or biological agents to regulate the body's autoimmune response and achieve tumor suppression.³ Tumor immunotherapy can improve immune function while killing tumor cells *in vivo*. A previous study found that the combination of traditional treatment and immunotherapy is better than single treatment, and it also provides a theoretical reference for future clinical treatment.⁴ Several studies indicate that low ionizing radiation can stimulate an adaptive response, including up-regulation of antioxidant responses, activation of apoptosis, and activation of the immune system to monitor neoplastic transformation.^{5,6} In addition, low-dose radiation (LDR) has been shown in animal models to delay spontaneous cancer, prevent chemocarcinogenic-induced cancer, prevent cancer metastasis, and extend the lifespan of individuals with the disease.⁷ Although

low ionizing radiation hormesis has been investigated in numerous studies, the optimal dose for promoting immune function remains unclear. Thus, the purpose of this article is to investigate the optimal dose of low ionizing radiation for liver cancer treatment and provide a theoretical basis for the adjuvant treatment of liver cancer.

Materials and methods

Animal model preparation

Twenty-five healthy New Zealand rabbits were selected (3–4 months old, 2–3 kg each; 12 males and 13 females) from the animal experiment center at Qiqihar Medical University (China). They were raised in the animal experiment center under a constant temperature of 15 to 25°C and a relative humidity of 40% to 70%. The drinking water and food for experimental animals were sterilized. The present study was approved by the Ethics Committee at Qiqihar Medical University of China, which agreed to the use of experimental animals for research (Approval number: 201907022).

Animal experiment reagents and instruments included depilatory cream (sodium sulfide and the distilled water 1:9), 75% ethanol solution, 1.5% pentobarbital sodium, 3% pentobarbital sodium, Anerdian, 0.9% isotonic saline, penicillin,³ VX-2 tumor tissue (provided by the Fourth Affiliated Hospital of Harbin Medical University, Harbin, China), enzyme-linked immunosorbent assay (ELISA) kits (Shanghai Future Industrial Co. Ltd., Shanghai, China),

microplate reader, centrifuges, incubator, digital color ultrasonic diagnostic instrument (Feiyinuo Technology Co. Ltd., Suzhou, China), Varian linac IX, slicing machine, optical microscope, and automatic hemocyte analyzer.

This animal study was performed in accordance with our university's guidelines and those of the molecular imaging laboratory at Qiqihar Medical University (China). All applicable international, national, and institutional guidelines for the care and use of animals were followed. The experimental animals were euthanized using an intravenous injection of 3% pentobarbital sodium solution through an ear vein.⁸ We made efforts to minimize the number of animals that were used.

Groups

Rabbits were divided into five groups (a control group and experimental groups 1–4) using a random number table in the Molecular Imaging Laboratory at Qiqihar Medical University. VX-2 tumor tissue was implanted into control group animals with no irradiation. Experimental groups 1 to 4 received VX-2 tumor tissue implantation. Fifteen days after tumor implantation, the rabbits in the four experimental groups received a single dose of whole-body irradiation using the Varian linear accelerator IX at the Third Affiliated Hospital of Qiqihar Medical University. Low ionizing radiation at doses of 25 mGy, 50 mGy, 75 mGy, or 100 mGy were used for the four study groups (experimental groups 1, 2, 3, and 4, respectively). We adhered to rigorous methodology for this classification.⁹

Preparation of VX-2 tissue fragments

Tumor tissue from the hind legs of tumor-bearing rabbits was surgically removed in a sterile environment, and the necrotic tissues were cut away. Then the tumor tissues were

cut into 25 pieces using ophthalmic scissors mixed with an equal amount of isotonic saline to make a tumor suspension for later use.

VX-2 tumor tissue implantation

Before surgery, the rabbits in the experimental and control groups were fasted for 24 hours and water was restricted for 8 hours. Anesthesia was injected (1.5% pentobarbital sodium; 2 mL/kg) into the ear vein. Then the anesthetized rabbit was fixed in the supine position on the laboratory bench. The upper abdomen was shaved and sterilized with aneridine. The rabbit's liver was located using a high-frequency B-ultrasound probe, and the prepared tissue was injected into the liver under B-ultrasonic guidance. After surgery, the experimental groups and control group were administered antibiotics, and their condition was monitored daily.

Blood chemistry

On day 4 after irradiation, 2 to 3 mL of peripheral blood was collected from each rabbit and white blood cell (WBC), red blood cell (RBC), lymphocyte (LY), and platelet (PLT) levels were measured in the laboratory department of the Second Affiliated Hospital at Qiqihar Medical University.

Detection of IL-4 and IFN- γ expression using ELISA

On day 4 after irradiation, 2 to 3 mL of peripheral blood was collected from each rabbit and centrifuged at $1084 \times g$ for 20 minutes. The upper level containing serum was taken, and the interleukin (IL)-4 and interferon (IFN)- γ levels were detected using ELISA kits (Shanghai Future Industrial Co. Ltd. Shanghai, China), in accordance with the manufacturer's instructions.

Immunoglobulin detection

On day 4 after irradiation, 2 to 3 mL of peripheral blood was collected from each rabbit, and the immunoglobulin (Ig)M and IgG levels were measured in the laboratory department in the Second Affiliated Hospital at Qiqihar Medical University.

Immune function detection

On day 14 after irradiation, a starch solution was injected into the rabbit's abdominal cavity, and on day 15 after irradiation, a 2% chicken erythrocyte suspension was injected into the rabbit's abdominal cavity. One hour later, peritoneal fluid was removed and stained using Wright–Giemsa dye. Macrophages phagocytosed the chicken erythrocytes, which were observed using a microscope under oil ($\times 100$). In each set of slides, ten microscope fields were selected to count 200 macrophages, and the number of macrophages that phagocytosed chicken erythrocytes and the average percentage of phagocytosis were calculated.

On day 15 after irradiation, the rabbits were sacrificed, and the spleens from each group were removed and weighed. The spleen index was calculated using the following equation: spleen index = spleen mass (g)/body weight (kg).

Micromorphology

On day 15 after irradiation, the rabbits were sacrificed, and liver tissue was removed for micromorphological observation. After the tumor tissues were removed, they were immediately fixed in a 10% formaldehyde solution for 24 hours at room temperature. The tumor tissue was washed and dehydrated for 5 hours under different ethanol concentrations and then cleared with different xylene concentrations. Tissues were processed for paraffin embedding at 58°C, and 4- μ m-thick slices were cut and placed

on smooth glass slides. Tissue samples were stained using hematoxylin and eosin, and observed differences between the tumor tissues in the experimental groups and the control group were observed under an optical microscope.

Data analysis

SPSS v.25.0 software (IBM Corp., Armonk, NY, USA) was used for statistical analysis in this experiment, and the data are presented as the mean \pm standard deviation. One-way analysis of variance (ANOVA) was used for the control and experimental groups, and $P < 0.05$ was considered to represent a statistically significant difference.

Results

General situation

Twenty-five rabbits were divided into five groups with five rabbits in each group (control group [0 mGy] and experimental groups 1, 2, 3, and 4 [25, 50, 70, and 100 mGy, respectively]). About 3 days after tumor tissue inoculation, rabbits in the control and experimental groups were in good physical condition, responded quickly to external stimuli, and they could eat and walk on their own. Fifteen days after inoculation, the rabbits had lost weight and were in poor physical condition, lying in the cage and not wanting to move. At this point, the rabbits in the experimental groups were subjected to low ionizing radiation. Twenty days after inoculation, the rabbits in the control group remained in poor physical condition, lying in the cage and not wanting to move; one of these rabbits refused to eat, lost a severe amount of weight, and died on day 24 after inoculation. The rabbits in the experimental groups were in good physical condition and able to respond quickly to external stimuli, and

they began to gain weight. No deaths occurred in the experimental groups. All rabbits were sacrificed on day 30 after inoculation. Upon autopsy, the control group rabbits had a foul odor in the abdominal cavity, and most of the liver was invaded by tumors; tumor metastasis had occurred in the abdominal organs, and some tissues were necrotic and purulent (Figure 1a). Rabbits in the experimental groups had no foul odor in the abdominal cavity where the liver was invaded by tumors, and a small part of the tumor appeared metastatic (Figure 1b).

Monitoring using B-ultrasonography

Liver tumors in rabbits in each group were detected every 3 days using B-ultrasound high-frequency probe (3.5 MHz). Seven days after tumor inoculation, hyperechoic masses with relatively clear boundaries were observed in the liver of rabbits in each group, indicating that tumor implantation was successful in all rabbits. Color

Doppler flow imaging showed a short rod-shaped blood flow signal inside the tumor. The tumor mass diameter was recorded on days 7, 15, and 25 after inoculation (Table 1). A one-way ANOVA showed that the differences between the 75 mGy group and other groups were not statistically significant.

Blood chemistry testing

The WBC, RBC, LY, and PLT levels in rabbit serum in the groups gradually increased as the irradiation dose increased. The 75-mGy group had the highest levels among the experimental groups (Table 2). The WBC, RBC, LY, and PLT levels in the 75-mGy group were significantly lower than the control group (0-mGy; $P < 0.05$), and these levels in the 75-mGy group were significantly higher than in the other experimental groups (25, 50, and 100 mGy groups; $P < 0.05$ for all).

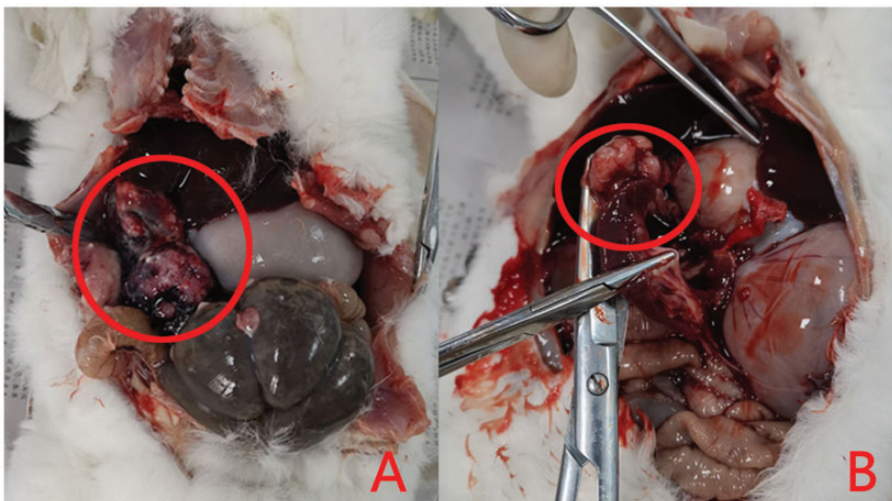


Figure 1. Abdominal anatomy of rabbits. (a) The tumor with abdominal cavity metastasis. Some tissues were necrotic and suppurative. (b) The liver was invaded by the tumor, and a small part of the tumor appeared metastatic.

Table 1. Comparison of tumor diameter.

Irradiation dose (mGy)	Day 7 (mm)	Day 15 (mm)	Day 25 (mm)
0	9.90 ± 0.51	17.44 ± 0.43	32.28 ± 0.72
25	11.21 ± 0.10	17.37 ± 0.47	31.32 ± 0.72
50	10.90 ± 0.47	17.44 ± 0.82	31.72 ± 0.21
75	10.29 ± 0.18	17.58 ± 0.96	30.47 ± 0.73
100	10.32 ± 0.62	18.57 ± 0.36	31.72 ± 0.18

Data are presented as the mean ± standard deviation.

Table 2. Comparison of blood chemistry analysis between groups.

Irradiation dose (mGy)	WBC ($\times 10^9$ cells/L)	RBC ($\times 10^{12}$ cells/L)	LY ($\times 10^9$ cells/L)	PLT ($\times 10^9$ cells/L)
0	7.72 ± 1.03 ^c	7.23 ± 0.97 ^b	3.53 ± 0.52 ^c	473.73 ± 85.45 ^b
25	6.78 ± 1.21 ^c	6.45 ± 0.72 ^b	2.52 ± 0.47 ^c	390.45 ± 57.67 ^b
50	7.34 ± 0.88 ^{bc}	6.55 ± 0.19 ^b	2.64 ± 0.67 ^b	421.32 ± 66.17 ^b
75	7.35 ± 1.12 ^a	6.78 ± 0.45 ^a	2.78 ± 0.65 ^a	434.03 ± 64.25 ^a
100	7.25 ± 0.84 ^b	6.36 ± 0.25 ^b	2.46 ± 0.46 ^{bc}	398.02 ± 74.44 ^b

Results followed by different letters in the same column indicate a significant difference within that column ($P < 0.05$). WBC, white blood cells; RBC, red blood cells; LY, lymphocytes; PLT, platelets.

Changes in IL-4 and IFN- γ secretion levels

The serum IL-4 and IFN- γ levels showed a gradually increasing trend for 0, 25, 50, and 75 mGy, while the IL-4 and IFN- γ levels were lower in the 100-mGy group than in the 75-mGy group. Among these results, the IL-4 and IFN- γ levels in the 75-mGy group were the highest (IL-4, 688.31 ± 54.37 pg/mL; IFN- γ , 15.83 ± 0.73 pg/mL; Table 3). Compared with the 75-mGy group, the IL-4 and IFN- γ levels in the other irradiation groups were significantly lower ($P < 0.05$).

Changes in the immunoglobulin level

The serum IgG and IgM levels showed a gradually increasing trend for 0, 25, 50, and 75 mGy, while the IgG and IgM levels were lower in the 100-mGy group compared with the 75-mGy group. The 75-mGy group showed the highest immunoglobulin levels (IgG, 6.32 ± 0.08 g/L; IgM, 0.66 ± 0.03 g/L; Table 4). Compared with the 75-mGy group, the IgG and IgM

Table 3. Comparison of IL-4 and IFN- γ secretion levels between groups.

Irradiation dose (mGy)	IL-4 (pg/mL)	IFN- γ (pg/mL)
0	480.16 ± 58.79 ^c	9.17 ± 0.71 ^c
25	516.21 ± 28.44 ^{bc}	10.83 ± 0.66 ^b
50	571.55 ± 46.23 ^b	12.44 ± 0.68 ^b
75	688.31 ± 54.37 ^a	15.83 ± 0.73 ^a
100	527.14 ± 22.36 ^{bc}	8.82 ± 0.34 ^{bc}

Results followed by different letters in the same column indicate a significant difference within that column ($P < 0.05$).

IL-4, interleukin 4; IFN- γ , interferon-gamma.

levels in the other groups were significantly lower ($P < 0.05$ for all).

Changes in macrophage phagocytic function

The nuclei were purple-red and the cytoplasm was light-red under the microscope, and phagocytosed chicken erythrocytes were observed (Figure 2). The amount of

Table 4. Comparison of IgG and IgM levels between groups.

Irradiation dose (mGy)	IgG (g/L)	IgM (g/L)
0	5.34 ± 0.05 ^e	0.53 ± 0.02 ^d
25	5.73 ± 0.04 ^d	0.57 ± 0.03 ^{cd}
50	5.88 ± 0.07 ^b	0.63 ± 0.05 ^b
75	6.32 ± 0.08 ^a	0.66 ± 0.03 ^a
100	5.62 ± 0.08 ^c	0.58 ± 0.02 ^{bc}

Results followed by different letters in the same column indicate a significant difference within that column ($P < 0.05$).

Data are presented as the mean ± standard deviation. Ig, immunoglobulin.

cells/L. Comparison of macrophage phagocytic function between groups.

macrophage phagocytosis showed a gradually increasing trend for 0, 25, 50, and 75 mGy, while the phagocytosis rate was lower in the 100-mGy group compared with the 75-mGy group. The 75-mGy group showed the most macrophage phagocytosis ($75.44 \pm 1.82\%$; Table 5). The 75-mGy group had significantly more macrophage phagocytosis compared with the other groups ($P < 0.05$ for all).

Changes in the spleen index

The spleen index showed an increasing trend for 0, 25, 50, and 75 mGy, while the spleen index was lower in the 100-mGy group compared with the 75-mGy group. The spleen index in the 75-mGy group was 7.61 ± 0.14 (Table 6). The 75-mGy group showed a significantly higher spleen index compared with the other groups ($P < 0.05$ for all).

Pathology examination results

Rabbits were sacrificed on day 15 after irradiation for pathology examination. The gross tumor specimens from the experimental groups showed gray tumor tissue with white with focal hemorrhage and necrosis.

The peripheral tumor capsule was intact, and the surrounding liver tissue showed macronodular cirrhosis.

The tumors were round or oval with an abundant blood supply, and they had a hard texture (Figure 3a). Liquefactive necrosis was observed after the incision was made. Under a low-magnification microscope, large amounts of fibrous tissue had proliferated and inflammatory cells had infiltrated the tumor tissue. Between the pseudolobules, the blood vessels were expanded and congested (Figure 3b). Carcinoma tissue migrated to the surrounding liver tissues.

Sinusoids were observed in the tumor tissue. Tumor cells in tumor tissues were arranged in a disordered manner, showing a striped shape or mass. Tumor cells varied in size and shape, the nuclei were large and deeply stained, and tumor giant cells and pathologic karyokinesis were visible (Figure 3c). Metastatic tumors were seen in other abdominal organs (Figure 3d). Using a high-magnification microscope, metastatic lymph nodes showed a large number of cancer cell nests, which were large and deeply stained and had large nuclei. The normal structure of the lymph nodes was completely destroyed. The rabbit tumor tissue specimens and microscopic sections were not significantly different between the experimental groups and the control group.

Discussion

Many studies have shown that LDR has an immune stimulation effect, which can promote immune function *in vivo* to achieve its tumor-inhibiting effect.¹⁰ Under normal circumstances, the immune system is in a homeostatic state. When the body is exposed to different doses of radiation, the number of immunocompetent cells, antibody-forming ability, and cytokine secretion level will significantly change,

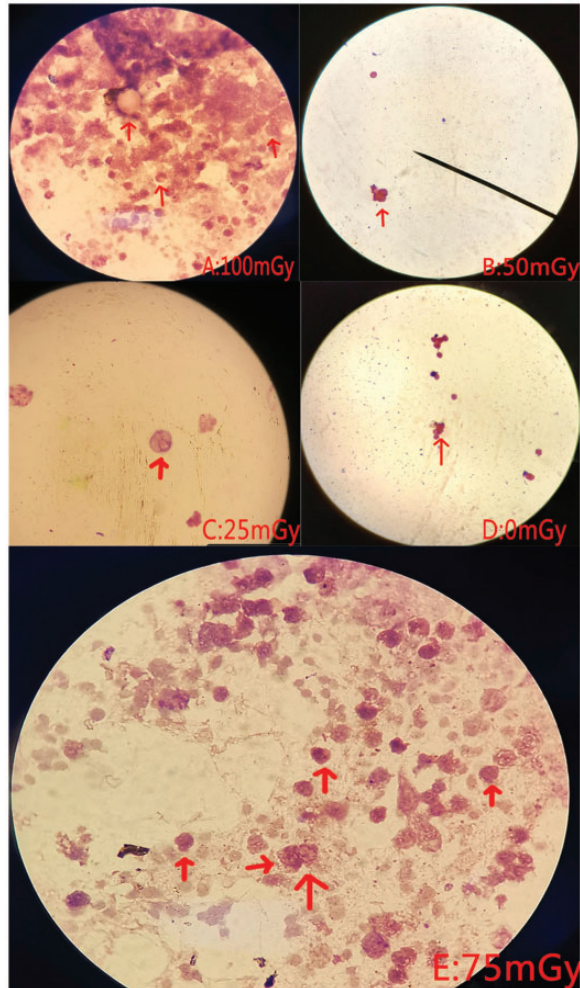


Figure 2. Microscopic images of chicken erythrocytes that were phagocytosed by macrophages. Some macrophages phagocytosed chicken erythrocytes.

which is important for the ionizing radiation immune effect.¹¹ LDR can enhance most immune responses, and its biological effect is essentially different from that of high-dose radiation.¹² The effects of LDR stimulation involve a series of cellular and molecular changes.¹³ Recent research has shown that the LDR immune effect mechanism involves many areas such as cell function, overall regulation, signal transmission, molecular expression, and gene regulation, which has received attention

from international organizations.¹⁴ Therefore, this study compared immunological indexes in experimental groups with different irradiation doses to determine the strength of the radiation hormesis in the immune system and to explore the optimal dose of low ionizing radiation to enhance immune function.

Immune function includes cellular immunity and humoral immunity. On the basis of the difference in secreted cytokines and mediated immune function, helper T

Table 5. The comparison of Macrophage phagocytic function between groups.

Irradiation dose (mGy)	Phagocytic percentage (%)
0	67.61 ± 2.02 ^c
25	68.84 ± 1.16 ^c
50	71.15 ± 1.24 ^b
75	75.44 ± 1.82 ^a
100	74.11 ± 1.41 ^b

Results followed by different letters in the same column indicate a significant difference within that column ($P < 0.05$).

Data are presented as the mean ± standard deviation.

Table 6. Comparison of the spleen index between groups.

Irradiation dose (mGy)	Spleen index (g/kg)
0	4.36 ± 0.21 ^d
25	5.62 ± 0.31 ^c
50	6.16 ± 0.44 ^b
75	7.61 ± 0.14 ^a
100	6.33 ± 0.41 ^b

Results followed by different letters in the same column source differ significantly within that column ($P < 0.05$).

Data are presented as the mean ± standard deviation.

lymphocytes can be divided into two main functional subsets, Th1 and Th2. Th1 cells secrete cytokines such as IL-2 and IFN- γ to induce macrophage activation and delayed hypersensitivity, and they participate in cellular immune regulation. Th2 cells mainly secrete cytokines such as IL-4 and IL-10, which induce the growth and differentiation of mast cells and eosinophils and participate in humoral immunity.¹⁵ The release of different cytokines in response to low ionizing radiation can enhance or inhibit the immune function and promote the initial transformation of T cells into helper T cells.¹⁶ IFN- γ is an important tumor necrosis factor, which can directly inhibit tumor cell proliferation, induce Th1 cell differentiation, activate macrophages, and increase

MHC-I and II expression, thereby inducing innate and acquired immune responses. In addition to directly elevating IFN- γ and IFN- α mRNA expression, low ionizing radiation can also induce TH1-type cytokine activation and enhance IL-12 gene transcription and protein expression, while IL-12 induces TH1 cells to produce IFN- γ .¹⁷ Mast cells and basophils, T cells, natural killer (NK) T cell subpopulations, and naive CD4+ T cells can produce IL-4, but Th2 cells are the most important producer of IL-4.¹⁸ IL-4 has a wide range of biological activities and can enhance the killing function of specific and non-specific cells. Its role in the immune response *in vivo* is complex. As the main inducer of Th0 cell differentiation to Th2 cells, IL-4 can regulate the balance of Th1/Th2 cells and participate in humoral immunity. However, other studies have found that IL-4 can also participate in cellular immunity by up-regulating IFN- γ and tumor necrosis factor (TNF)- α expression.¹⁹ Therefore, low ionizing radiation may achieve an anti-tumor effect by up-regulating IL-4 and IFN- γ secretion levels to regulate the humoral and cellular immunity in response to the tumor. This mechanism needs to be further explored.

In this experiment, IL-4 and IFN- γ levels in the four experimental groups (25, 50, 75, and 100 mGy) increased compared with the control group (0 mGy). The IL-4 and IFN- γ levels in the 75-mGy group increased significantly compared with the other experimental groups (25, 50, and 100 mGy; $P < 0.05$ for all). B cells play a role in humoral immunity by producing immunoglobulin, and IgG and IgM are common indexes of immune function.¹⁹ There are few studies on the effect of low ionizing radiation on humoral immunity. Currently, it is believed that low ionizing radiation, as a special weak antigen, can stimulate repeated polyclonal activation of B cells and induce the formation of immunoglobulin to enhance

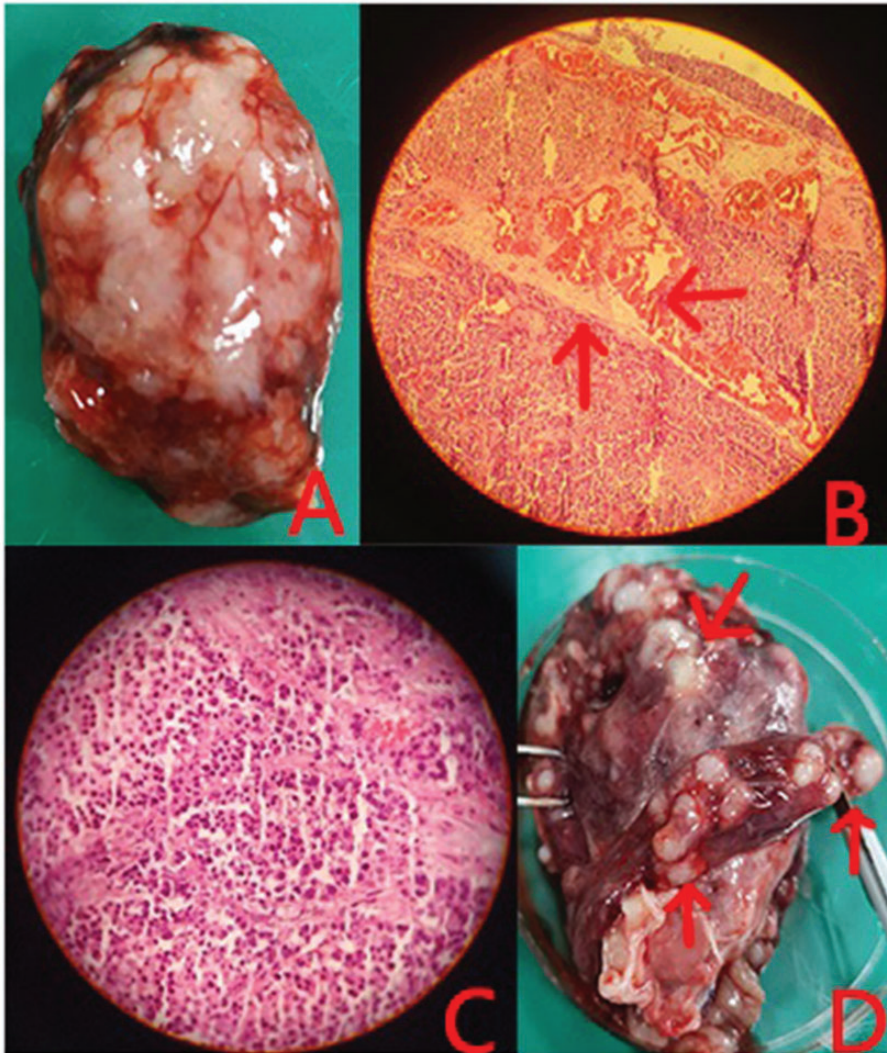


Figure 3. (a) A gray-white tumor with hemorrhagic necrosis. (b) Under a light microscope (10× magnification), there was a large amount of fibrous tissue, infiltrative inflammatory cells, and dilated and congested blood vessels in the tumor tissue. (c) Under a light microscope (40× magnification), there was a disordered arrangement of tumor cells. (d) Tumor tissue that had metastasized to other organs. The tumor tissue is off-white in color and nodular in appearance.

humoral immune function.²⁰ A large number of IgG and IgM antibodies with high affinity can be produced after being stimulated by low ionizing radiation.¹⁴ IgG and IgM in the experimental groups (25, 50, 75, and 100 mGy) were significantly higher than those in the control group

(0 mGy), showing a gradually increasing trend, which suggests that low ionizing radiation can improve immunoglobulin levels in patients with tumors. However, the effects of low dose ionizing radiation on the body are complex and variable, including both radiation hormesis and

harmful effects. The 100-mGy group showed a downward trend compared with the 75-mGy group ($P < 0.05$), suggesting that 75 mGy may be the optimal dose to stimulate the immune system.

Macrophages are an important indicator immunity *in vivo*. They are widely distributed in the abdominal cavity, liver, kidney, muscle, bone, adipose tissue, and blood. Their functions are phagocytosis, sterilization, secretion of inflammatory factors, and tumor suppression, which are important roles in the immune response.²¹ Macrophages play an important role in non-specific immunity, and participate in *in vivo* anti-infection, anti-tumor, and immune regulation processes. The strength of the phagocytosis can affect immune function.²² This experiment showed that the phagocytosis rate of macrophages increased significantly in all four experimental groups compared with the control group. This could be because X-ray-stimulated macrophages secrete nitric oxide (NO), which indirectly improved the phagocytosis function of macrophages, thereby inhibiting tumor cell growth in the body.²² The 75-mGy group showed the most significant improvement, suggesting that 75 mGy may be the optimal dose to strengthen the immune system.

The spleen is a peripheral immune organ. The spleen contains a variety of mature lymphocytes and is involved in the immune response, and the spleen reflects the immune function of the body to a certain extent.²³⁻²⁶ In this study, after low ionizing radiation, the cell proliferation kinetics in rabbits changed, and the proliferation characteristics changed adaptively. The cell cycle may subsequently be shortened and proliferation may be accelerated.²⁷ In this manner, the immune function of the body was improved. Compared with the control group, the spleen index of the rabbits in the 75-mGy group was significantly higher ($P < 0.05$).

The results showed that the immune indexes were significantly improved, which can confirm radiation hormesis after low ionizing radiation. These results also suggested the optimal dose of low ionizing radiation that induced radiation hormesis in the immune system. The results showed that the immune indexes in the 75-mGy group were significantly higher than in the other irradiation dose groups. It has been reported in literature that activation of effector T cells was the key to enhance the immune response to low ionizing radiation hormesis.²⁸ Different surface molecules and cytokines were expressed by effector T cells after different doses of low ionizing radiation. Therefore, 75 mGy was the optimal dose for low ionizing radiation to induce radiation hormesis in the immune system. The mechanism may be that low ionizing radiation at a dose of 75 mGy can maximize the number of immune active cells (e.g., T lymphocytes, B lymphocytes, NK cells) and that cytokine and antibody formation can be regulated by LDR.

This study has some limitations including a small sample size and limitations due to the kits. Future studies with a larger sample size should be conducted concurrently to confirm the optimal dose of low ionizing radiation to improve immune function from multiple angles and factors.

Conclusion

The effect of low ionizing radiation on the immune system is mainly manifested in a series of changes in cellular and molecular levels such as the number of immune cells, the secretion level of cytokines and immunoglobulins, the formation of antibodies, and the regulation of cytokines, which ultimately leads to positive regulation of the body's immune function. Among different doses of low ionizing radiation, 75 mGy was the optimal dose to improve immune function.

This experiment also innovatively applies the anti-tumor effect of low ionizing radiation to adjuvant treatment of animal liver cancer models. The results provide serological evaluation and serological data on the immune effects of ionizing radiation and radiotherapy for malignant tumors.

Author contributions

Y.Z. and H.R.: study concept and design and data analysis and interpretation. M.L.: drafted the manuscript. Y.Z.: magnetic resonance device operation and image data analysis. Q. Y.: sample acquisition and data and statistical analysis.

Acknowledgments

We would like to thank Qiqihar Medical Center Animal Center for helping us to construct the rabbit model, the Molecular Imaging Laboratory of Qiqihar Medical University for daily monitoring of the model rabbits, the Third Affiliated Hospital of Qiqihar Medical University for Varian linac IX support, and the Second Affiliated Hospital of Qiqihar Medical University for use of their immunoglobulin detection device.


Declaration of conflicting interest

The authors declare that there is no conflict of interest.

Funding

This work was supported by the University Students Innovation and Entrepreneurship Training Project of Heilongjiang Province (201911230012) and the Qiqihar Medical Academy Project of 2019 (QMSI2019L-22).

ORCID iD

Liguo Hao  <https://orcid.org/0000-0001-6102-4493>

References

- Chen W, Zheng R, Baade PD, et al. Cancer statistics in China, 2015. *Ca Cancer J Clin* 2016; 66: 115–132. DOI:10.3322/caac.21338.
- Torre LA, Freddie B, Siegel RL, et al. Global cancer statistics, 2012. *Ca Cancer J Clin* 2015; 65: 87–108. DOI:10.3322/caac.21262.
- Feng L, Qin L, Guo D, et al. Immunological mechanism of low-dose priming radiation resistance in walker-256 tumor model mice. *Exp Ther Med* 2017; 14: 3868–3873. DOI: 10.3892/etm.2017.4975..
- Wang Y. Advances in hypofractionated irradiation-induced immunosuppression of tumor microenvironment. *Front Immunol* 2021; 11: 612072. DOI: 10.3389/fimmu.2020.612072.
- Gori T and Münzel T. Biological effects of low-dose radiation: of harm and hormesis. *Eur Heart J* 2012; 33: 292–295. DOI:10.1093/eurheartj/ehr288.
- Betlazar C, Middleton RJ, Banati RB, et al. The impact of high and low dose ionizing radiation on the central nervous system. *Redox Biol* 2016; 9: 144–156. DOI:10.1016/j.redox.2016.08.002
- Scott B. Low-dose-radiation activated natural protection and LNT. *Health Phys* 2011; 100: 377–339. DOI:10.1097/hp.0b013e3182059442
- Hudzik B, Nowak J, Szkodzinski J, et al. Discordance between body-mass index and body adiposity index in the classification of weight status of elderly patients with stable coronary artery disease. *J Clin Med* 2021; 10: 943. DOI: 10.3390/jcm10050943.
- Ghadimi M, Foroughi F, Hashemipour S, et al. Decreased insulin resistance in diabetic patients by influencing Sirtuin1 and Fetuin-A following supplementation with ellagic acid: a randomized controlled trial. *Diabetol Metab Syndr* 2021; 13: 16. DOI: 10.1186/s13098-021-00633-8..
- Wennerberg E, Lhuillier C, Vanpouille-Box C, et al. Barriers to radiation-induced in situ tumor vaccination. *Front Immunol* 2017; 8: 229. DOI: 10.3389/fimmu.2017.00229..
- Gao J, Pan Y, Xu Y, et al. Unveiling the long non-coding RNA profile of porcine reproductive and respiratory syndrome virus-infected porcine alveolar macrophages. *BMC Genomics* 2021; 22: 177. DOI: 10.1186/s12864-021-07482-9..

12. Cheng GH, Wu N, Jiang DF, et al. Increased levels of p53 and PARP-1 in EL-4 cells probably related with the immune adaptive response induced by low dose ionizing radiation in vitro. *Biomed Environ Sci* 2010; 23: 487–495. DOI:10.1016/S0895-3988(11)60012-3
13. Schwartz JL. Variability: The common factor linking low dose-induced genomic instability, adaptation and bystander effects. *Mutat Res* 2006; 616. DOI:10.1016/j.mrfmmm.2006.11.016
14. Vaes RDW, Hendriks LEL, Vooijs M, et al. Biomarkers of radiotherapy-induced immunogenic cell death. *Cells* 2021; 10(4): 930. DOI: 10.3390/cells10040930.
15. Wang Z, Wu JL, Zhong F, et al. Upregulation of proBDNF in the mesenteric lymph nodes in septic mice. *Neurotox Res* 2019; 36: 540–550. DOI: 10.1007/s12640-019-00081-3.
16. Glady G. Clinical efficacy of implementing bio immune(g)ene medicine in the treatment of chronic asthma with the objective of reducing or removing effectively corticosteroid therapy: a novel approach and promising results. *Exp Ther Med* 2018; 15: 5133–5140. DOI: 10.3892/etm.2018.6019.
17. Fagiolo E and Toriani-Terenzi C. IFN-gamma and TNF-alpha production in gamma-irradiated blood units by mononuclear cells and GVHD prevention. *Transfus Apher Sci* 2002; 27: 225–231. doi:10.1016/s1473-0502(02)00069-1
18. Gómez V, Mustapha R, Ng K, et al. Radiation therapy and the innate immune response: clinical implications for immunotherapy approaches. *Br J Clin Pharmacol* 2020; 86: 1726–1735. DOI: 10.1111/bcp.14351.
19. Xiong J, Lin YH, Bi LH, et al. Effects of interleukin-4 or interleukin-10 gene therapy on trinitrobenzenesulfonic acid-induced murine colitis. *BMC Gastroenterol* 2013; 13: 165. DOI: 10.1186/1471-230X-13-165..
20. Du Y, Sun H, Lux F, et al. Radiosensitization effect of AGuIX, a gadolinium-based nanoparticle, in non-small cell lung cancer. *ACS Appl Mater Interfaces* 2020; 12: 56874–56885. DOI: 10.1021/acsami.0c16548.
21. Storzynsky Q, Hitt MM. The impact of radiation-induced DNA damage on cGAS-STING-Mediated immune responses to cancer. *Int J Mol Sci* 2020; 21: 8877. DOI: 10.3390/ijms21228877.
22. Iwamori M, Tanaka K, Adachi S, et al. Enhanced fucosylation of GA1 in the digestive tracts of X-ray-irradiated mice. *Glycoconj J* 2017; 34: 163–169. DOI: 10.1007/s10719-016-9746-3.
23. Tubin S, Khan MK, Gupta S, et al. Biology of NSCLC: Interplay between cancer cells, radiation and tumor immune microenvironment. *Cancers (Basel)* 2021; 13: 775. DOI: 10.3390/cancers13040775.
24. Lee EK, Kim JA, Kim JS, et al. Activation of de novo GSH synthesis pathway in mouse spleen after long-term low-dose x-ray irradiation. *Free Radic Res* 2013; 47: 89–94. DOI:10.3109/10715762.2012.747678I
25. Kovalchuk IP, Golubov A, Koturbash IV, et al. Age-dependent changes in DNA repair in radiation-exposed mice. *Radiat Res* 2014; 182: 683–694. DOI:10.1667/rr13697.1
26. Reiko I, Laura PH, Susan MG, et al. Late effects of exposure to ionizing radiation and age on human thymus morphology and function. *Radiat Res* 2017; 187: 589–598. DOI:10.1667/RR4554.1
27. Yang K, Hou Y, Zhang Y, et al. Suppression of local type I interferon by gut microbiota-derived butyrate impairs antitumor effects of ionizing radiation. *J Exp Med* 2021; 218: e20201915. DOI: 10.1084/jem.20201915.
28. Deng L, Liang H, Xu M, et al. STING-dependent cytosolic DNA sensing promotes radiation-induced type I interferon-dependent antitumor immunity in immunogenic tumors. *Immunity* 2014; 41: 843–52. DOI: 10.1016/j.immuni.2014.10.019.